The Thesis Committee for Matthew Niles Wallack
Certifies that this is the approved version of the following thesis:

Investigations of the C8S3 J-aggregate

APPROVED BY
SUPERVISING COMMITTEE:

Supervisor:

David A. Vanden Bout

Keith J. Stevenson

Investigations of the C8S3 J-aggregate

by

Matthew Niles Wallack, B.S.; B.S.; M.S.

Thesis

Presented to the Faculty of the Graduate School of

The University of Texas at Austin

in Partial Fulfillment

of the Requirements

for the Degree of

Master of Arts

The University of Texas at Austin

December 2012

Dedication

This work is dedicated to my family, friends, and loved ones. Thank you for your help, faith, and support. I couldn't have done this without you.

Acknowledgements

The constant praise and support of my friends and family have bolstered my confidence in the good times and helped me through the bad. I had never thought that I would still be in school at the age of 30, but I also had never dreamt that I would have achieved 4 degrees by the end of my time at school. I can't thank all of you enough for everything you have done for me. When life gets me down, you are the ones I think of to make everything better, you have my most heartfelt thanks.

Abstract

Investigations of the C8S3 J-aggregate

Matthew Niles Wallack, M.A.

The University of Texas at Austin, 2012

Supervisor: David A. Vanden Bout

This research project entails analyses of both alcoholic route C8S3 J-aggregate bundles and the interactions of a polyethylene glycol additive with alcoholic route C8S3 J-aggregates. First, the C8S3 J-aggregate bundles are characterized by both polarized and non-polarized spectroscopy methods. Orientation of the tubular bundled molecular complex was achieved, depending on the experiment, through a combination of flow cell experiments and cover slip deposited sample analysis. Next, isolated alcoholic route C8S3 J-aggregates were investigated using a polyethylene glycol (PEG) additive which has been shown, through absorbance and fluorescence emission spectroscopy, to selectively and reversibly remove the outer wall of the J-aggregate tubule. Spectroscopic analyses have indicated that the addition of a PEG additive left behind an in-tact inner wall tubule without the use of oxidizing agents, a feat never before accomplished with the C8S3 monomer.

Table of Contents

List of Figures

CHAPTER 1: BUNDLED C8S3 J-AGGREGATES

Introduction

J-aggregates have a unique set of physical, optical, and electronic properties which have made them a subject of scientific interest for the past 75 years.[1] When a critical concentration of J-aggregate monomer dye is placed into an aqueous solvent, the dye spontaneously self-assembles into a supramolecular structure which can be monitored by UV-Vis spectroscopy. Self-assembly of the monomers into the suprastructure causes a red shift and narrowing of the absorbance transitions as compared to the transitions of the monomer.[2, 3, 4, 5] Studies on the electronic properties of tubular J-aggregates have revealed them to be efficient at energy collection and transfer, effectively acting as model systems for light harvesting complexes. [6, 7, 8, 9, 10, 11]

The J-aggregate monomer used in this study was 3, 3'- bis(2-sulfopropyl) - 5, 5', 6, 6'- tetrachloro - 1, 1 '-dioctylbezimidacarbocyanine (C8S3), its structure is shown in Figure 1.[12] When left to aggregate under aqueous conditions, the C8S3 monomers aggregate to form a double walled tubular structure.[13] Figure 2A-C illustrates how individual C8S3 monomers assemble during the aqueous aggregation progress of an isolated J-aggregate tubule.[12] Under aqueous conditions, each monomer molecule orients its 8 carbon hydrophobic region toward the hydrophobic regions of other C8S3 monomers in solution. Minimization of aqueous exposure to the hydrophobic region causes the formation of a double walled tubular structure.[14] The solvent exposed walls

of this tubular structure are hydrophilic regions and the non-exposed area between the walls make up the hydrophobic region. This double walled tubular structure bears a resemblance to light harvesting antennae molecules found in naturally occurring photosynthetic systems.[12, 15, 16] This structural resemblance has made tubular J-aggregates the subject of recent scientific interest.

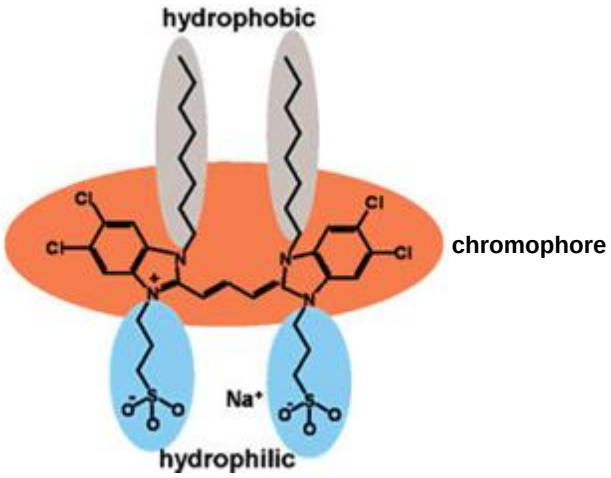

Figure 1. Structure of the C8S3 monomer. The 8 carbon hydrophobic chain is shown in grey. The hydrophilic sulfopropyl groups are shown in blue. The chromophore is shown in orange. (Image courtesy of Lyon et al)[12]

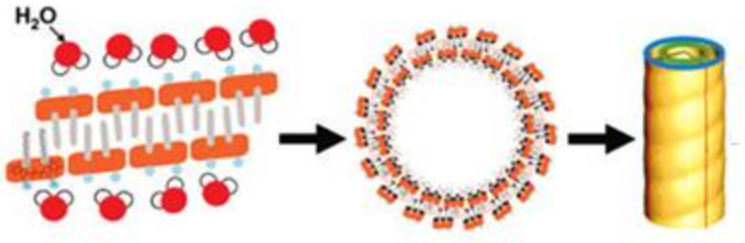

Figure 2. A: Amphiphilic orientation of C8S3 monomers dispersed in aqueous media. Grey blocks represent the hydrophobic 8 carbon chains of each respective monomer, blue circles represent the hydrophilic sulfopropyl groups, orange blocks represent chromophores of each respective monomer. Water molecules are represented by red and white dots, oxygen and hydrogen atoms respectively. (Images courtesy of Lyon et al)[12]

B: Double walled tubular structure of a C8S3 J-aggregate as seen edge on.

C: Double walled tubular structure of a C8S3 J-aggregate as viewed from the side. The green circle represents the chromophores comprising the inner wall, whereas the blue circles represent the chromophores comprising the outer tubule wall.

Almost every study to date has focused on experiments utilizing freshly created J-aggregate samples, performing experiments within a week of initial aggregation from the monomer. Older samples have been regarded with a passive curiosity, but have otherwise not been extensively studied.[12, 17, 18, 19] When stored in the dark, to avoid photo chemical degradation, the absorption spectrum of the J-aggregate solution changes. Figure 3 shows absorption spectra of a freshly prepared alcoholic route J-aggregate sample (blue) overlaid on top of a 6 month old J-aggregate sample (red). With respect to freshly prepared alcoholic route C8S3 J-aggregates, the two prominent narrow transitions of the older sample transform into a broad peak of higher energy than either of the fresh sample transitions, and a narrow peak of lower energy than either of the fresh sample

transitions. Cryo-TEM of the multi-week old solutions has shown that the spectroscopic changes are correlated to the physical bundling of the individual J-aggregate tubules in solution.[18] These older samples will be referred to as "bundled J-aggregates."

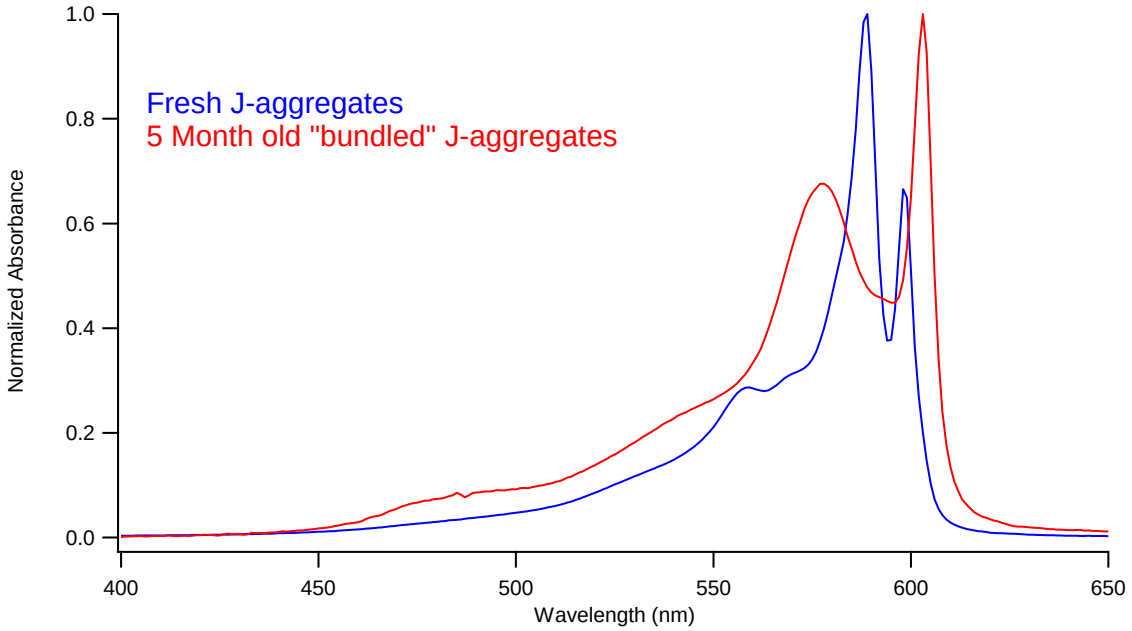

Figure 3. Normalized UV-Vis absorption spectra of freshly prepared C8S3 J-aggregates (blue) and 5 month old "bundled" C8S3 J-aggregates (red).

This portion of this thesis focuses on the study of the fundamental characteristics of C8S3 J-aggregate bundles. We have observed that bundled C8S3 J-aggregates have a greater longevity than their freshly prepared counterparts, lasting for several months before any spectral absorbance changes are observed. Freshly prepared J-aggregates, however, can start exhibiting spectral absorbance changes in as few as 2 days after sample creation. Cryo-TEM images of bundled J-aggregates reveal that the bundles can form by each J-aggregate tube laying parallel to each other or by the J-aggregate tubes

twisting around each other.[18] The clustered formation of these bundled J-aggregates resembles the close packed natural state of light harvesting antennae found within the chlorosomes of purple bacteria.[16] The study of bundled J-aggregates as synthetic analogues of the clustered natural light harvesting antennae within a chlorosome will provide insight into the optical and electronic effects of bundling on natural light harvesting systems.

The ability to vary the absorbance characteristics of these light harvesting molecules through the close packing of individual tubules into a bundle, while still maintaining the long range energy transfer properties of isolated J-aggregates, is one of the driving forces behind this research.[20] Optimization of such systems can only take place after we understand the complex effect that bundling has on the monomer dipoles contained within this J-aggregate system.

Experimental

Alcoholic Route J-aggregate and J-aggregate bundle creation

Creation of J-aggregate bundles initially involved making *alcoholic route* J-aggregates. Alcoholic route J-aggregates were created by first making a 2.92 mM stock solution of C8S3 monomer dispersed in methanol. 130 μL of monomer stock solution was added to 500 μL of 18.3 MΩ water in a 0.5 dram vial covered with foil. The vial was then gently rocked for 5 seconds and left to stand in the dark for 24h, after which time, 500 μL of 18.3 MΩ water was added to the vial to stabilize the solution, creating a final monomer concentration of 0.336 mM. Absorbance spectra were then acquired and compared to spectra of freshly prepared C8S3 J-aggregates to spectrally confirm formation of isolated J-aggregates. Once the J-aggregates had been formed, they were left to sit in the dark at room temperature for several weeks, during which time they spontaneously assembled into J-aggregate bundles.

The creation of direct route J-aggregates is similar to that of the alcoholic route J-aggregates, except that the monomer is not initially stabilized in methanol. Instead the monomer is directly added to a vial of water, and stirred vigorously for 24 h in order to induce solvation. The monomer solution is then left to stand in the dark to aggregate. Direct route J-aggregate bundles then form over the course of several weeks. Direct route J-aggregates were not used in this work, except by way of comparison to other bundled J-aggregate data.

Fluorescence Emission Scans

Fluorescence emission spectra of bundled C8S3 J-aggregates were acquired using a Fluorolog 1 Fluorimeter. Excitation and emission slits were set to 1 mm, giving a final resolution of 1.8 nm. Measurements were taken utilizing a 0.1 mm thick quartz sample cell in the front faced geometry and a detector integration time of 250 ms. The excitation was set to 560 nm to ensure that the main transitions of the absorbance spectrum could be investigated without interference from scattering.

RCA Cleaning

Glass cover slips utilized in AFM and NSOM experiments were cleaned using a RCA cleaning procedure. Glass cover slips were placed into a solution containing equal parts of the following 3 solutions: reagent grade Ammonium Hydroxide, 30% concentrated Hydrogen Peroxide, and 18 MΩ high purity water. The solution was heated to 60 °C to initiate the reaction, and left to sit for 1 h. After 1 h the cover slips were extracted from the RCA mixture, rinsed with deionized water and left to dry.

Sample Deposition

AFM and NSOM samples were deposited on RCA cleaned cover slips by the drop flow technique. A dry cleaned cover slip was held at a 60° angle while a 50 μL aliquot of sample was deposited on the top edge of the slide and allowed to flow down to the bottom of the slide. The excess sample solution was removed from the slide by placing the bottom most corner of the slide onto a clean kimwipe and allowing the wicking action to remove excess sample solution. The sample deposited cover slip was then left to dry in the dark for 30 min.

AFM

Atomic force microscopy (AFM) experiments were acquired on a Multimode™ AFM utilizing Vista Probes Tap 300 cantilevers.

NSOM

Near-field scanning optical microscopy (NSOM) images of J-aggregate bundles were acquired using a modified Aurora Topometrix NSOM with in-house produced NSOM probes.[21] A 20 mW 532 nm diode laser was used as the excitation source. The excitation source was circularly polarized to insure minimal polarization bias from the excitation source. Circular polarization was achieved using a 532 nm λ/2 plate and a 532 nm λ/4 plate. The wave plates were rotated until each detector registered equal counts from the excitation source during the alignment process. After alignment a 550 nm long pass filter was installed. Upon leaving the sample, light was passed through the long pass filter to block photons generated by the excitation source and pass photons generated by the sample. The light was then passed through a 50/50 polarizing beam splitter, into the X-axis and Y-axis emission detectors, a Perken Elmer Photon Counting Module and an EG&G Photon Counting Module, respectively. The sample was rastered across the fiber optic tip using a piezoelectric stage. Sample-tip distance was maintained through a shear force feedback loop which measured the dampening of a 100 kHz tuning fork attached to the aluminum coated fiber optic tip. The schematic diagram of the NSOM can be seen in Figure 4.

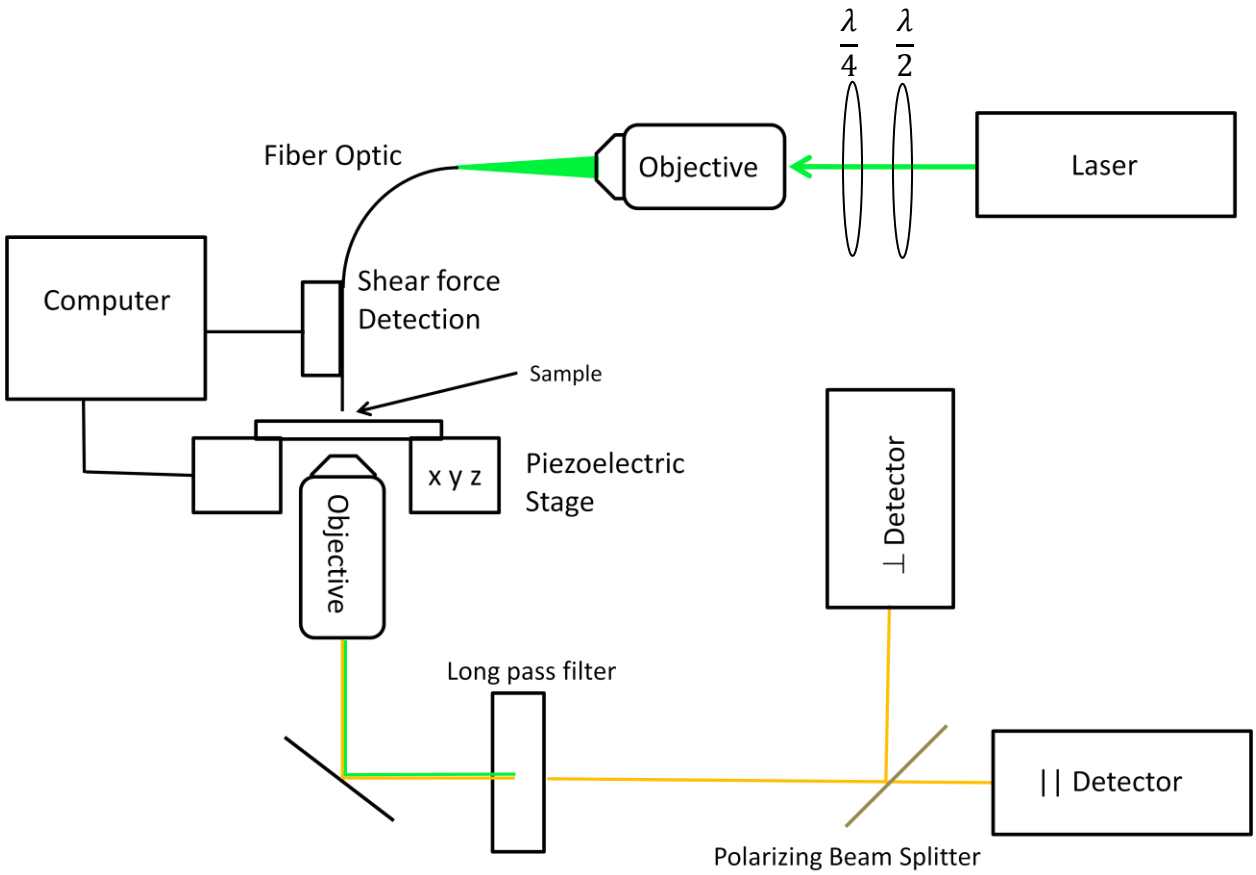

Figure 4. Schematic drawing of the near-field scanning optical microscope (NSOM) and its component parts. Both objectives had a magnification of 10x. Quarter and half wave plates are labeled above.

Fluorescence Excitation Anisotropy Scans

Fluorescence excitation anisotropy scans of J-aggregate bundles were acquired on a Fluorolog 3 fluorimeter utilizing a front faced geometry and a 0.1 mm thick quartz sample cell. The excitation was scanned from 550-606 nm (16501.65 – 18181.82 cm^{-1}), utilizing an emission wavelength of 610 nm (16393.44 cm^{-1}). Excitation and emission slits were set to 2 nm and the integration time was set to 0.2 seconds.

Absorption Spectroscopy Scans

All absorption spectra were acquired at room temperature using an HP8453A diode array spectrophotometer. Polarized absorption spectra were obtained using a linear polarizer oriented at 0° and 90° with respect to the orientation of the sample through a flow cell. Orientation of the sample was achieved utilizing a flow rate of 75 mL/minute generated by a Master Flex L/S pump, a rate proven to be adequate for polarized absorbance measurements of freshly prepared isolated J-aggregate solutions. The path length of all quartz sample cells and flow cells was 0.1 mm. Absorption spectra of the bundled J-aggregate samples were acquired immediately before and after flowing the sample through the cell to insure no sample degradation had occurred for the duration of the experiment. The absorption spectra before and after the experiment proved to be identical.

Curve Fitting

Curve fitting was performed using the Multipeak Fitting 2 application in the IGOR Pro analysis software. Experimental absorbance spectra and experimental reduced linear dichroism spectra were fit to Lorentzian curves.

Discussion

Absorption Spectra of J-aggregate Bundles

Tubular C8S3 J-aggregates are primarily created in two ways, in the absence of alcohol and in the presence of alcohol, referred to as direct route and alcoholic route J-aggregates respectively. Figure 5 shows absorbance spectra of methanol dispersed C8S3 monomer and freshly prepared alcoholic route C8S3 J-aggregates. The absorbance spectrum of the C8S3 monomer (blue) reveals a single low intensity broad transition with maxima located at 520 nm. J-aggregates produced by the alcoholic route (red) have absorbance spectra which contain a broad low intensity high energy tail and two intense absorbance transitions with maxima located at 589 and 599 nm. Literature shows that absorbance spectra of J-aggregates produced by the direct route contain a broad low intensity high energy tail and three predominant absorbance transitions with maxima locations at 570, 585, and 605 nm.[18] It has been shown that the spectral differences between the J-aggregate creation routes are caused by differences in the monomer packing of each macrostructure, resulting in different tubule diameters and geometries for the two J-aggregate creation routes. The geometry of the monomers within the macrostructure of the J-aggregate determines the energy coupling between the inner and outer tubular walls. The coupling causes the differences in the J-aggregate absorbance spectra. [18, 22]

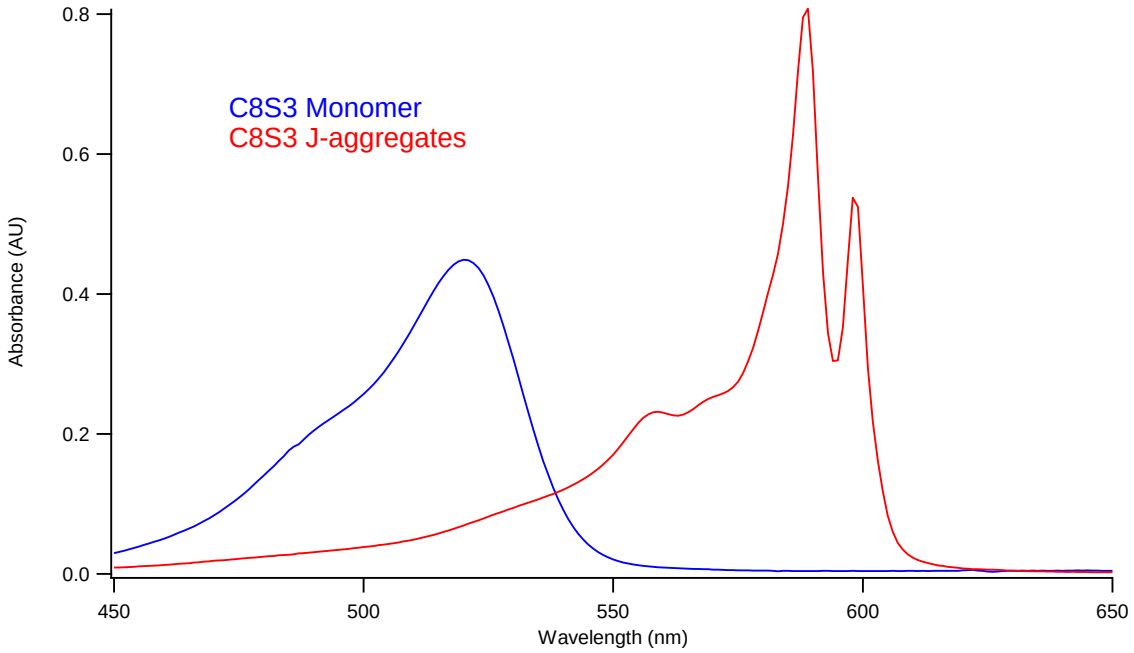

Figure 5. UV-Vis absorption spectra of methanol dispersed C8S3 monomer (blue) and alcoholic route C8S3 J-aggregates (red).

The absorption spectrum of an alcoholic route C8S3 J-aggregate bundled sample was acquired and compared to known absorption spectra of a direct route C8S3 J-aggregate bundled sample found in the literature. Figure 6 shows the alcoholic route C8S3 J-aggregate bundled absorption spectrum, which was left to sit in the dark for 6 months. The bundled J-aggregate spectrum shown in Figure 6 reveals two prominent absorption transitions, a narrow transition at 603 nm and a broad transition at 578 nm. It should be noted that the two methods of initially forming J-aggregates, alcoholic route and direct route, both yield the same qualitative spectral shape once bundling has occurred. *Collectively, the absorption spectra indicate that the characteristic shape of bundled C8S3 J-aggregates was reproducible and independent of the initial creation*

route of J-aggregates, direct or alcoholic. With respect to tubular aggregates, the narrow shape of the peak at 603 nm is a strong indicator that at least one tube of the initial double walled tubular system has remained relatively unchanged after the bundling process has occurred. Whereas the broad transition at 578 nm gives an indication of significant disorder within the high energy transition.

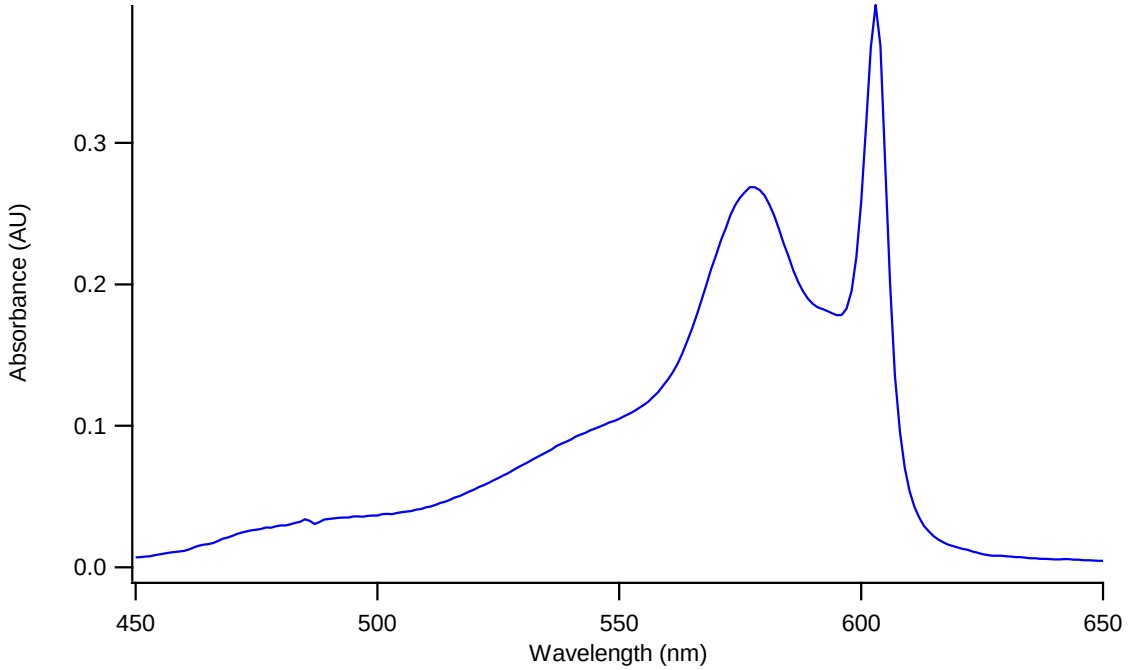

Figure 6. UV-Vis absorption spectrum of alcoholic route C8S3 J-aggregate bundles.

Emission

Figure 7 shows fluorescence emission spectra of a bundled J-aggregate sample normalized to the excitation source. The excitation wavelength was set to 560 nm to ensure that the main transitions of the absorbance spectrum could be investigated for emission without interference from scattering. The J-aggregate emission scan shows a

single sharp emission transition at 603 nm in resonance, having no stokes shift, with the low energy transition of the absorbance scan. The high energy region of the single prominent emission transition is asymmetric, indicating the presence of a low intensity transition near 590 nm, the same location as the outer wall transition in isolated alcoholic route J-aggregate tubules. This minor transition can also be seen in the alcoholic route bundled J-aggregate absorbance spectrum as a minor shoulder between the 570 nm and 603 nm peaks, shown in Figure 6. The low intensity transition could indicate the presence of isolated J-aggregates within the bundled sample solution.

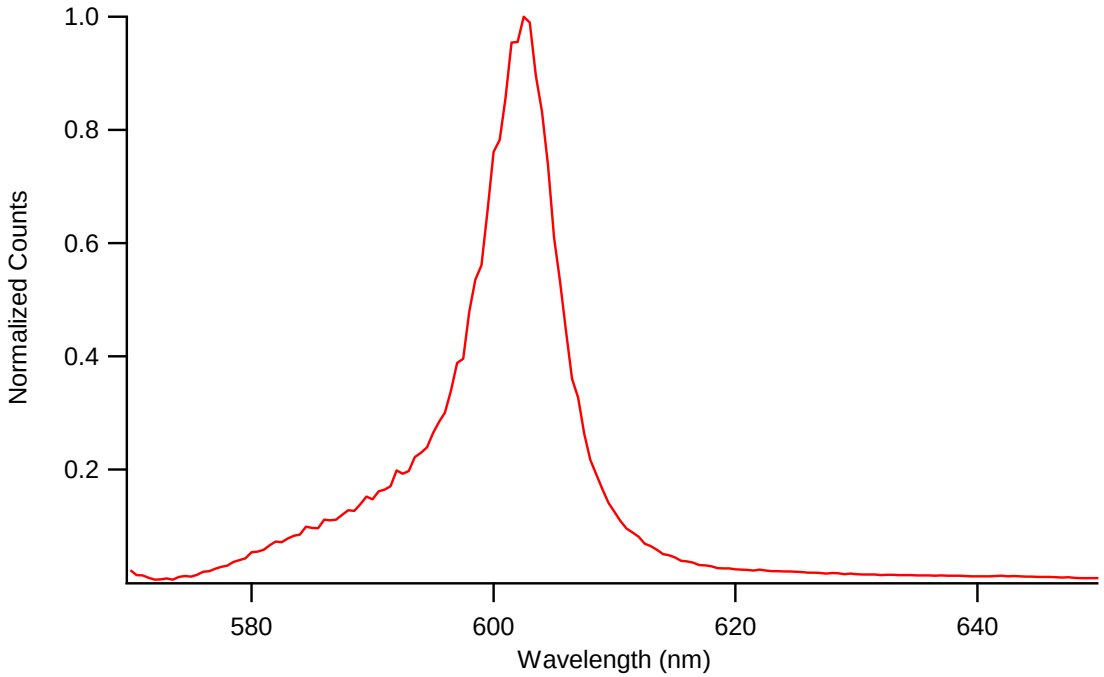

Figure 7. Normalized fluorescence emission spectrum of a bundled C8S3 J-aggregate sample. The excitation was set to 560 nm.

AFM

Topographical analysis of dried bundled J-aggregate samples was performed by atomic force microscopy (AFM) as shown in Figure 8. The 5x5 μm micrograph reveals intertwining bundles of J-aggregates joined together to form larger J-aggregate bundles. The thickest of the bundles have height maxima of 26 nm above the background, while the smaller bundles have heights of 13 - 19 nm above the background. Low height broken J-aggregate fragments can be seen in the image (F), indicating that some unbundled J-aggregates may still exist in the bundled sample. The linear arrangement of the fragmented J-aggregates indicates that the tubes were intact when they were deposited on the cover slip and fragmented during the drying process. The irregularly spaced fragmentation of the low height J-aggregate could have been caused by structural defects in the separated aggregate, but this was not the focus of this work.

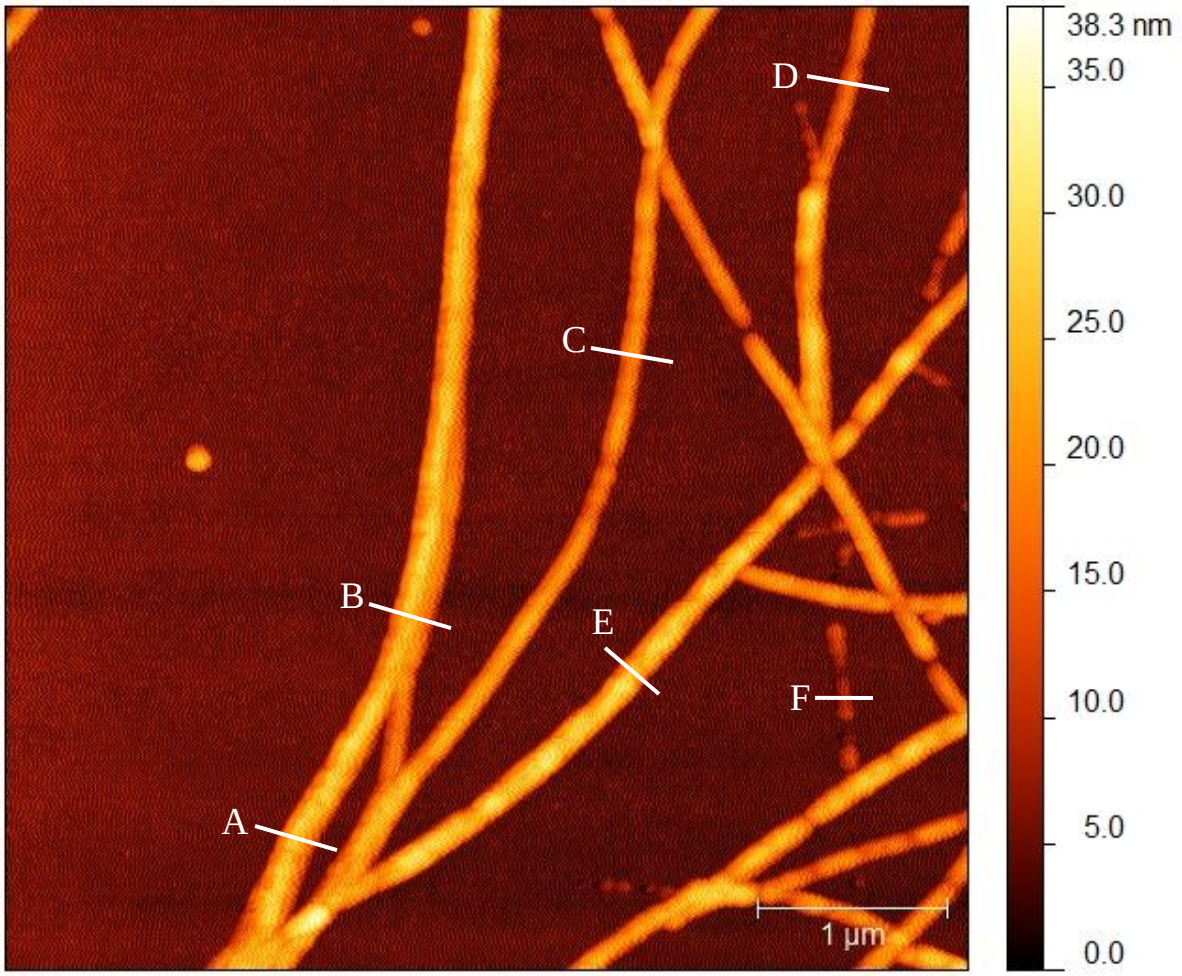

Figure 8. A 5x5 µm AFM micrograph of a bundled C8S3 J-aggregate sample. The background subtracted height maxima of the bundled J-aggregates are as follows: A. 26 nm, B. 26 nm, C. 19 nm, D. 13 nm, E. 25 nm, and F. 4 nm

Polarized NSOM

Figure 9 shows correlated topographical, dichroism, X-axis and Y-axis emission images of the same bundled J-aggregate sample. The image labeled "X counts" shows tube like structures corresponding to bundled J-aggregates polarized horizontally with respect to the image. Bundled tubules which are oriented horizontally show more

emission than tubules aligned vertically in the “X counts” image. The image labeled “Y counts” shows the same bundled tubular structures as seen in “X counts” polarized vertically with respect to the image instead of horizontally. Tubules oriented vertically in the “Y counts” image have a higher intensity than tubules oriented horizontally. A vertically and horizontally oriented tubule, which is visible in each image, have been marked with white and green ovals, respectively. Though the intensity of each tubule is greatest in the image corresponding to its directional orientation, horizontal for “X counts” and vertical for “Y counts”, the other tubule is still visible in the opposing image. This is because each tube has a mix of horizontal or vertical character, neither being perfectly vertical or horizontal in orientation.

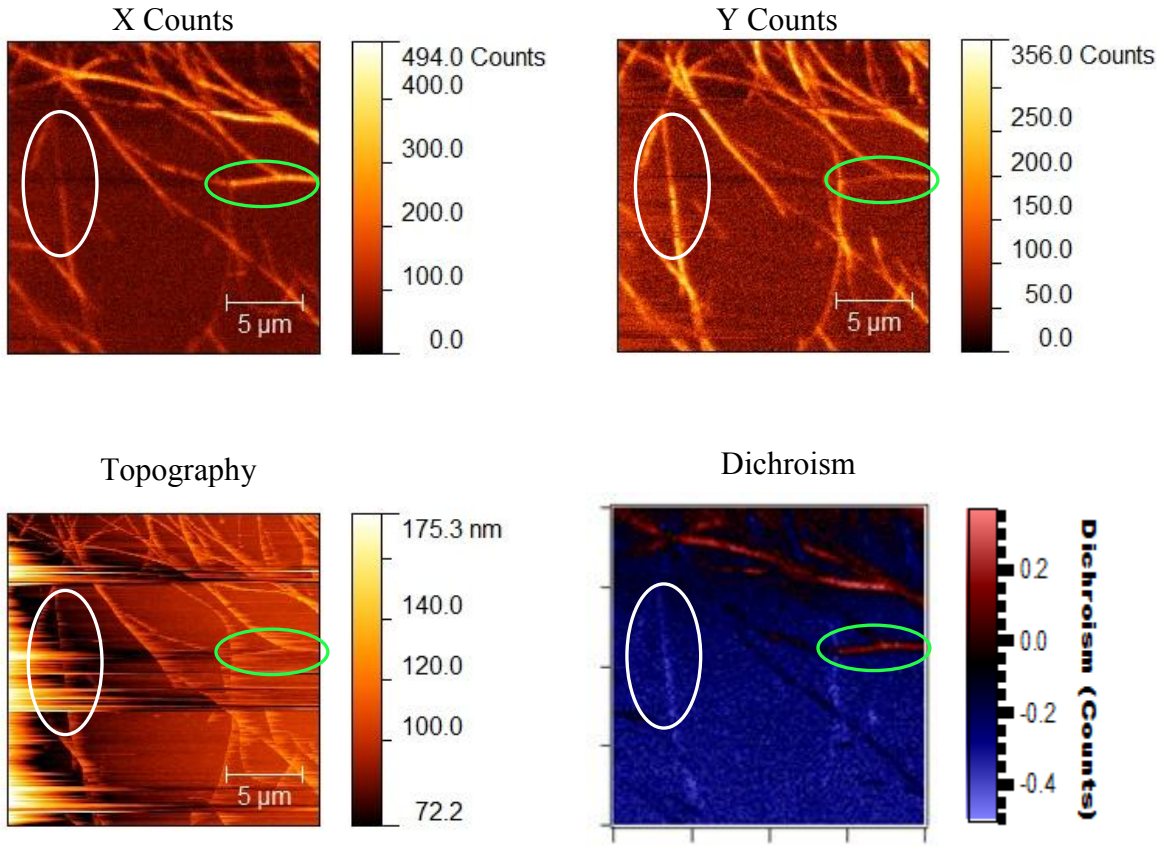

Figure 9. Correlated X-axis, Y-axis, Topography, and Linear Dichroism images of a 20x20 µm C8S3 bundled J-aggregate sample. The white oval denotes a bundled tubule that is oriented in the vertical direction and is correlated in all 4 images. The green oval, correlated in all 4 images, denotes a bundled tubule that is oriented in the horizontal direction. Streaks in the topography image were caused by low gain settings which caused the tip to momentarily lose contact with the sample.

The image labeled "Topography" shows a topographical image corresponding to the tubules found in the two emission images. Though the images are correlated, low gain settings which manage the constant tip to sample distance, caused imperfections in the topographical NSOM images. However, high resolution AFM images which were

previously discussed in this work have already addressed the topographical features of a typical bundled J-aggregate sample.

One method to observe the polarization of an oriented molecule is linear dichroism. A linear dichroism image was generated by subtracting the Y-axis emission image from the X-axis emission image. Positive values were shown in red and negative values were shown in blue. Though the dichroism image reveals a Y-axis bias, (blue background) it can be seen that the predominant emission of the J-aggregate bundle is aligned along the long axis of the tubular bundle. Horizontal bundles appear red and vertical bundles appear blue. Fluorescence emission spectra of bundled J-aggregate samples have revealed that the only emission transition emanating from a bundled J-aggregate sample is the 603 nm transition, a transition which is resonant in both absorption and emission spectra. The NSOM images give a physical interpretation to the polarization of the emission peak that cannot be achieved with certainty, using only a bulk sample measurement. The 603 nm emission peak was found to be polarized along the long axis of the tubular bundle. These results are supported by fluorescence anisotropy data and sample oriented reduced linear dichroism experiments presented later in this work.

Polarized absorbance

Figure 10 shows polarized absorbance spectra of a C8S3 J-aggregate bundled sample acquired using a flow aligned sample cell. The spectrum is plotted on an energy scale in wavenumbers. The parallel absorbance spectrum (Red) shows peaks with

maxima at 16584 cm^{-1} [603 nm] and 17331 cm^{-1} [577 nm]. The perpendicular absorbance spectrum (Blue) shows transitions with maxima at 16584 cm^{-1} [603 nm] and 17301 cm^{-1} [578 nm]. The transition at 16584 cm^{-1} is very narrow and common to both parallel and perpendicular spectra, though the intensities of the peaks differ the maxima locations stay the same. The results of the fluorescence NSOM scans indicated that the 16584 cm^{-1} transition is polarized along the long axis of the bundled tubule. This suggests that the bundles are not perfectly aligned with the direction of the flow through the cell.

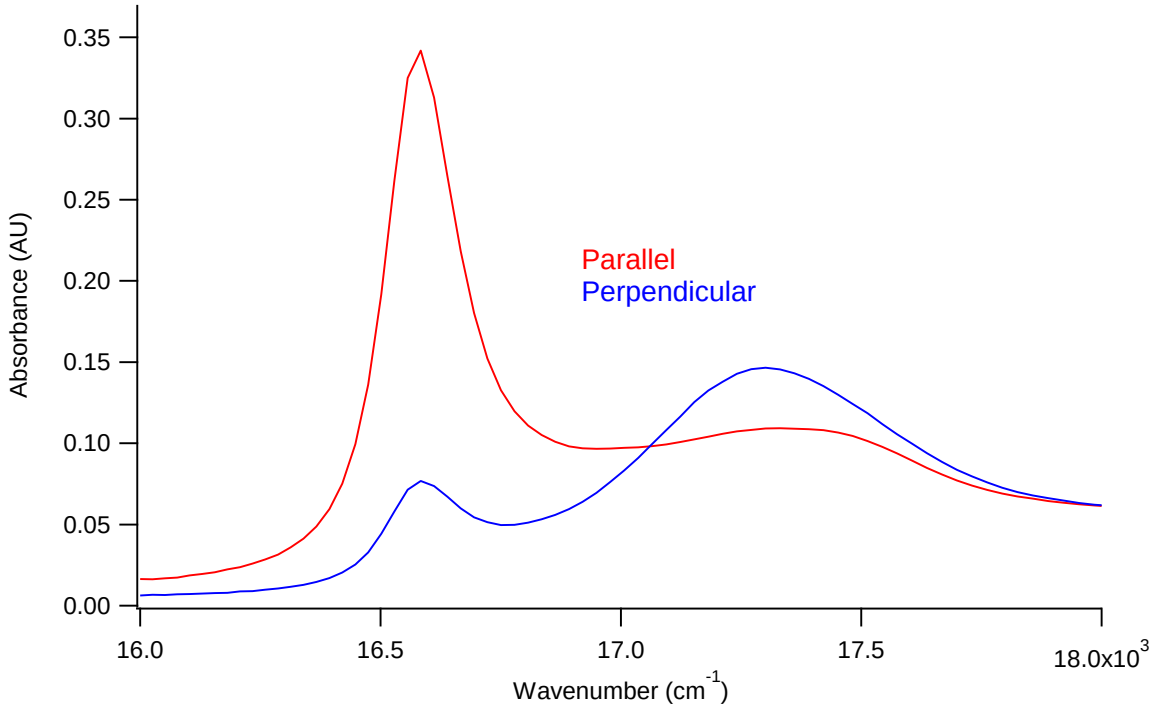

Figure 10. Parallel (red) and Perpendicular (blue) UV-Vis absorption spectra of a bundled C8S3 J-aggregate sample. A flow cell pumping at a rate of 75 mL/minute was used to orient the long axis of the sample in the direction of the flow. A linear polarizer was oriented at 0° and 90° with respect to the flow to obtain parallel and perpendicular absorbance spectra, respectively.

The transition with maxima at 16584 cm^{-1} does not change maxima locations with respect to parallel and perpendicular spectra. This suggests that any changes in maxima locations are not caused by changes in intensity or instrumental variation. The broad transitions of the parallel and perpendicular spectra have transition maxima that differ by 30 cm^{-1}. This 30 cm^{-1} separation indicated that there were at least 2 absorbance transitions hidden within the broad high energy peak of the isotropic absorbance spectrum, if not more. The two maxima found in the high energy region indicate that this broad transition is comprised of a continuum of peaks instead of a single broad transition. The predominant polarization of the narrow transition (16584 cm^{-1}) is parallel, whereas the predominant polarization of the broad continuum is perpendicular.

The experimental reduced linear dichroism (LDr) was calculated utilizing the parallel and perpendicular absorption spectra in the equation shown below. Where "$A_{||}$" is the parallel absorbance spectrum, "$A_{\perp}$" is the perpendicular absorbance spectrum, and "A" represents the isotropic absorbance spectrum. [23]

$$LDr = \frac{LD}{A} = \frac{A_{||} - A_{\perp}}{A} = \frac{A_{||} - A_{\perp}}{\left(A_{||} + 2A_{\perp}\right) * \left(\frac{1}{3}\right)}$$

An overlay of the normalized isotropic absorbance spectrum and experimental reduced linear dichroism (LDr) is shown in Figure 11. The experimental reduced linear dichroism reveals a strong parallel polarization at 16556 cm^{-1} (604 nm), a weak broad perpendicular polarization at 17271 cm^{-1} (579 nm), and an isotropic tail that extends into the high energy region of the spectrum. When compared to transitions of the isotropic

absorbance, the high energy perpendicular transition of the LDr appears to be narrower and has less perpendicular character than would be expected from a peak containing a single polarized transition. This is an indication that the high energy transition is in reality, a continuum of several overlapping transitions of opposing polarized character, parallel and perpendicular. The low intensity of the perpendicular transition, in the LDr, combined with the broad nature of the high energy peak of the non-polarized absorbance spectrum, indicates that there is a high degree of overlapping isotropic character which reduces the contribution of the perpendicular transition in the LDr.

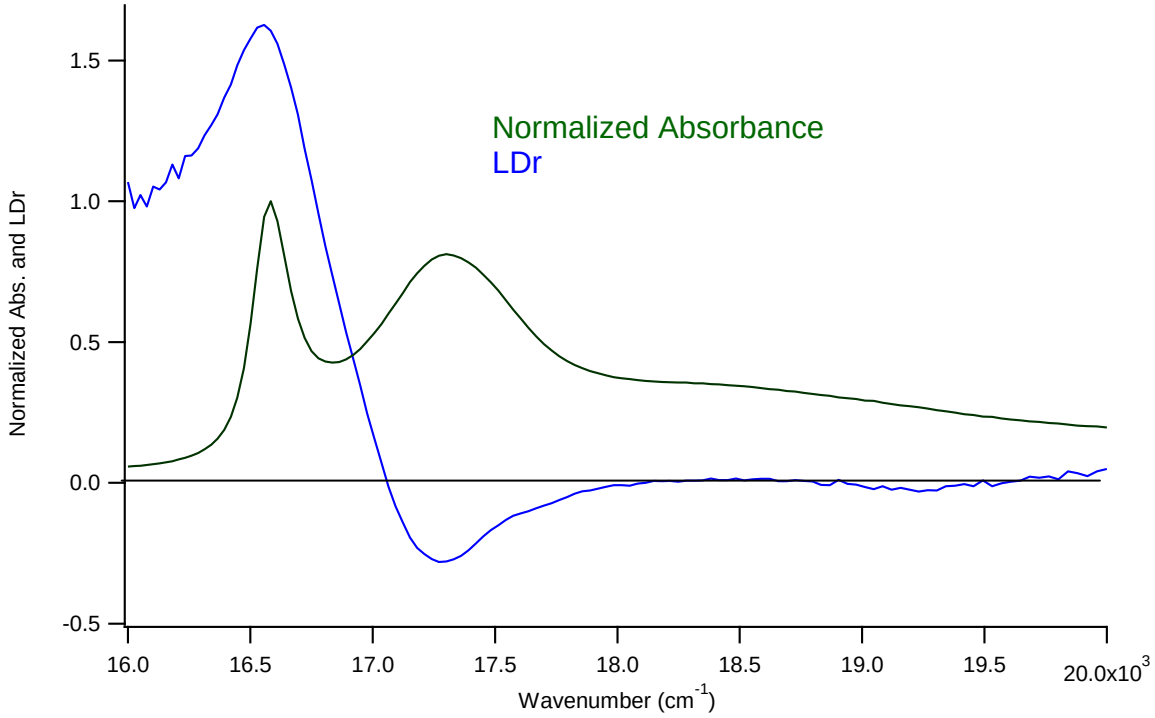

Figure 11. Normalized UV-Vis spectra (green) of a C8S3 bundled J-aggregate sample. Reduced linear dichroism (blue) of a flow oriented C8S3 bundled J-aggregate sample. The sample was oriented using a flow cell pumping at a rate of 75 mL/min. A black line has been added to denote a linear dichroism of zero.

Simultaneous curve fitting of the isotropic absorbance spectrum and the experimental LDr was performed to gain insight into the polarization identities of each of the bundled J-aggregate absorbance transitions. Each absorbance transition was represented by a Lorentzian curve and assigned a polarization identity: parallel, perpendicular, or isotropic. Efforts were made to create the simplest model possible utilizing the fewest transitions to simultaneously describe the isotropic absorbance and the LDr using a single set of transitions. The individual transitions created from the isotropic absorbance curve fit were utilized in the fit linear dichroism equation shown below; where $P_{||}$ is a parallel transition, $P_{\perp}$ is a perpendicular transition, and P_{iso} is an isotropic transition.

$$LDr\ Fit = \frac{(3 * P_{||} - (3/2) * P_{\perp})}{(P_{||} + P_{\perp} + P_{iso})}$$

Simultaneous curve fits of the absorption and LDr spectra are shown in Figures 12A and 12B. The simultaneous fit utilized 4 transitions labeled 0 through 3 which were polarized in the following ways: Peak 0 parallel, Peak 1 parallel, Peak 2 perpendicular, and Peak 3 was isotropic in polarization. The peaks of the fit were labeled according to the numbering system of the IGOR curve fitting program. The narrow transition of the isotropic absorbance spectrum, centered at 16587 cm^{-1} (603 nm), is represented by a single parallel transition labeled peak 0. The low intensity parallel transition, labeled Peak 1, is positioned at 16900 cm^{-1} (592 nm). This low intensity transition is similar in

energy to the parallel outer wall transition of isolated C8S3 alcoholic route J-aggregates, indicating that there may be individual non-bundled J-aggregates in the sample solution. The single perpendicular transition of the simultaneous fit, Peak 2, favors the lower energy side of the broad continuum, whereas the high energy side appears to have significant isotropic character, Peak 3. The fit was restricted to 4 total transitions rather than adding in a 5^{th} perpendicular peak to represent the unresolved transition in the interest of keeping the model simple.

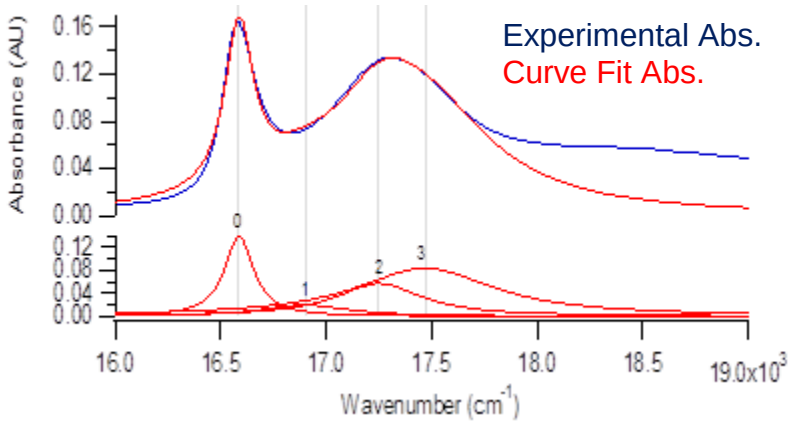

Figure 12A. Top: Experimental UV-Vis absorption spectrum of a bundled C8S3 J-aggregate sample (blue). Summation curve fit of the bundled C8S3 J-aggregate sample (red). **Bottom:** Four peaks which make up the summation curve fit, representing transitions found within the bundled J-aggregate spectrum. The Lorentzian peaks have been assigned with the following polarization assignments: Peak 0 = Parallel, Peak 1 = Parallel, Peak 2 = Perpendicular, and Peak 3 Isotropic.

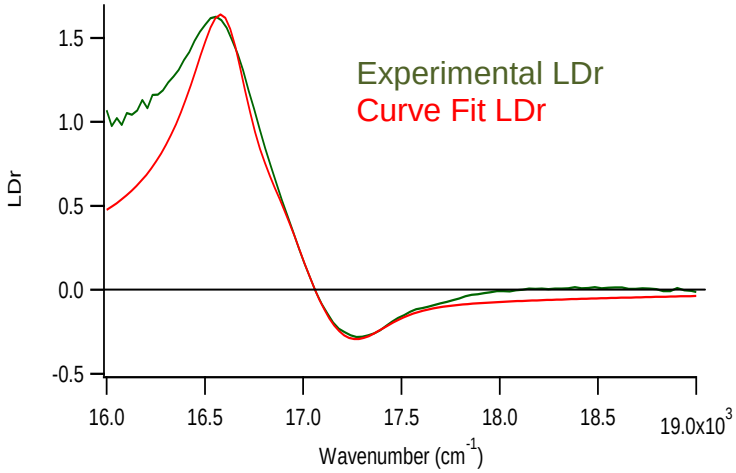

Figure 12B. Experimental reduced linear dichroism of a bundled C8S3 J-aggregate sample (green). Curve fit of the experimental linear dichroism created utilizing the polarizations of the transitions found at the bottom of Figure 12A (red). A black line has been added to denote a linear dichroism of zero.

The deviation of the curve fit LDr from the experimental LDr in the 16000 – 16500 cm^{-1} region is caused by an overabundance of parallel character originating from minor differences in the baseline of the parallel and perpendicular absorption spectra. As

the deviation originates from a minor baseline difference in the experimental data, this deviation can be ignored. The curve fit was restricted to areas of the LDr with significant parallel or perpendicular character. A single isotropic transition was added to compensate for the large amount of isotropic overlap inherit on the high energy side of the perpendicular transition. The deviation of the absorbance fit from the experimental data in the 17700-19000 cm^{-1} range originates from the limits placed upon this fit. Since the addition of more isotropic transitions into this simultaneous fit would significantly impact only the isotropic peak, it was felt that further complicating the model would be superfluous.

The simplest optical selection rules for tubular aggregate systems state that there should be one parallel absorbance transition and one perpendicular absorbance transition for each wall of a tubular system.[24, 25] It should be noted that the high intensity parallel transition of the curve fit does have an accompanying perpendicular peak, Peak 0 (16587 cm^{-1}) and Peak 2 (17250 cm^{-1}) respectively. The low intensity parallel peak of the curve fit, Peak 1 (16900 cm^{-1}), does not appear to have an accompanying perpendicular peak, showing a deviation from the selection rules. The most likely reason for this deviation is that the low intensity parallel transition has an accompanying unresolved parallel transition hidden within the broad continuum of peaks. It is unknown whether Peak 1 originates from the bundled J-aggregate itself, or if it originates from the outer wall of a single isolated J-aggregate, whose perpendicular transition could not be resolved from the broad continuum.

AFM micrographs of broken low height tubules in a bundled J-aggregate sample support the idea of non-bundled damaged J-aggregates in solution. The presence of broken separated J-aggregates could explain the low intensity parallel transition (16900 cm^{-1}) found in the fit of the absorbance and is supported by the fluorescence emission data. The remaining low intensity transitions associated with the selection rules in the bundled J-aggregate sample are likely lost to the background of more intense overlapping transitions.

Excitation Anisotropy

Figure 13 shows a fluorescence excitation anisotropy spectrum of a bundled C8S3 J-aggregate sample. The emission was set to 610 nm (16393 cm^{-1}) to capture as much of the excitation spectrum as possible without interference from scattering. The equations utilized to calculate the experimental excitation anisotropy are shown below where "I" represents the emission detected at 610 nm. The subscripts "H" and "V" represent the orientations of linear polarizers positioned to affect the excitation light source and emission coming from the sample. The first letter in the two letter subscript pair represents the excitation polarization, whereas the second letter represents the emission polarization, H for horizontal, V for vertical. The G-factor "G" is a correction factor for the detector bias with respect to vertically and horizontally polarized light, measured using an isotropic fluorescent dye. Measurements were taken by acquiring data at each wavelength from each polarization and then moving onto the next wavelength, this step by step measurement minimizes the effect of photo chemical degradation on the spectra.

$$G = \frac{I_{HV}}{I_{HH}} \qquad\qquad R = \frac{I_{VV} - GI_{VH}}{I_{VV} + 2 * GI_{VH}}$$

The experimental anisotropy of a bundled J-aggregate sample is shown in Figure 13. The range of the anisotropy scan encompassed every resolvable transition location found within the bundled isotropic J-aggregate absorption spectrum. The positive anisotropy centered at 16667 cm^{-1} corresponds to the parallel transition found near the same location in the spectrum of the reduced linear dichroism. The slightly negative anisotropy in the high energy region could indicate that perpendicular polarization dominates the high energy region of the spectrum. The lack of the rounded curve shape within the 17000-17500 cm^{-1} in the excitation anisotropy, which is present in the reduced linear dichroism, suggests that the perpendicular domination is a result of instrumental bias as opposed to originating from several low intensity perpendicular polarized transitions, thus creating a flat perpendicular tail. The polarization assignments gathered from the excitation anisotropy of bundled C8S3 J-aggregates are consistent with the polarization assignments initially detected in the reduced linear dichroism spectra and NSOM images of the same sample.

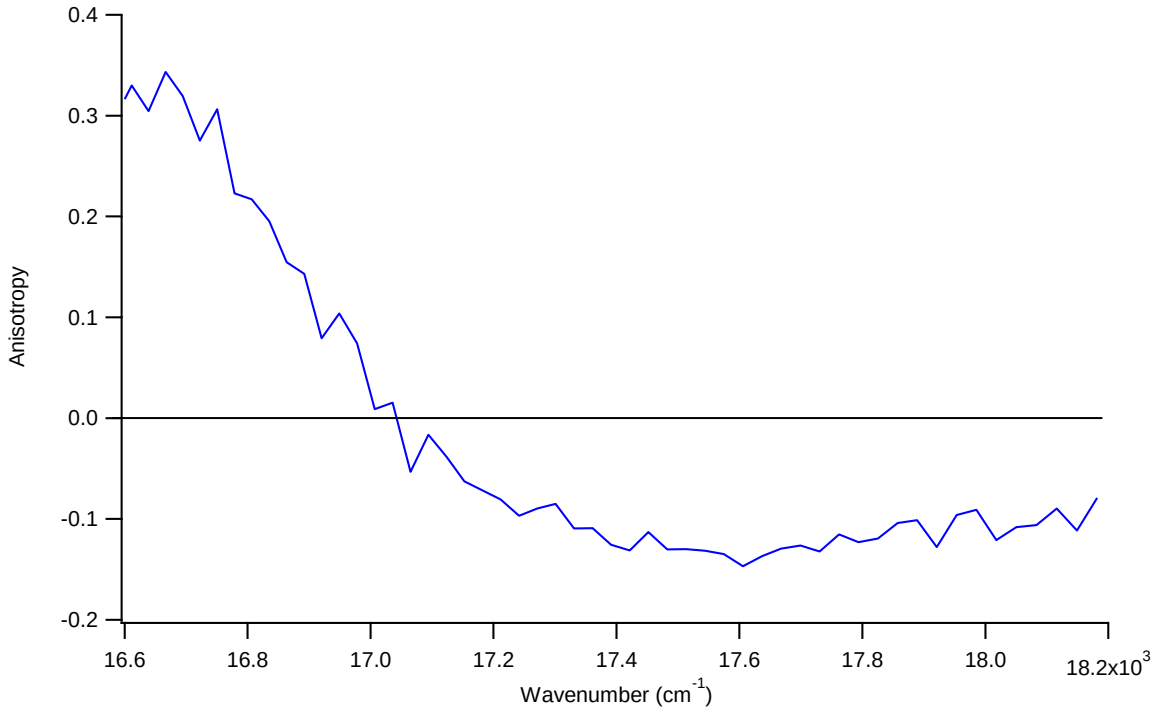

Figure 13. Excitation anisotropy spectrum of a C8S3 bundled J-aggregate. Emission was set to 610 nm (16393.44 cm^{-1}). A black line has been added which denotes an anisotropy of zero.

Conclusions

The work shown in this section has presented a thorough characterization of the bundled C8S3 J-aggregate. Bundled J-aggregates represent a robust form of the C8S3 J-aggregate system. Bundled C8S3 J-aggregates have been shown to be stable over time with absorption spectra that are highly reproducible regardless of the initial method of J-aggregate creation, alcoholic route or direct route. Emission scans of the bundled sample have shown that the narrow low energy absorbance transition (~603 nm or 16584 cm^{-1}) maintains the quality of resonant fluorescence found in isolated C8S3 J-aggregates. Polarization experiments have shown the narrow low energy transition to be polarized parallel to the long axis of the tubule. The broad high energy transition of the absorbance spectrum (578 nm or 17301 cm^{-1}) was shown to have a predominantly perpendicular polarization. The broad high energy absorbance transition was shown to be a continuum of parallel and perpendicular transitions explaining the broad nature of the peak as well as its significant degree of isotropic character originating from disorder in the system.

Outlook

The work presented in this section detailed the study of alcoholic route C8S3 J-aggregate bundles. The further study of J-aggregate bundles could lead to a better understanding of the clustered natural light harvesting antennae found in nature. The ability to quench the fluorescence of the high energy transition, thereby stopping energy transfer along the tubule, could lead to more innovative usages of this synthetic light harvesting energy transferring molecular complex.

CHAPTER 2: POLYETHYLENE GLYCOL C8S3 J-AGGREGATES

Introduction

Researchers have studied several aspects of J-aggregate spectra and structure with respect to monomer modification, substituting a wide variety of functional groups into the hydrophobic and hydrophilic regions of the monomer. Other experiments have incorporated the use of solvent additives into J-aggregate solutions during the aqueous assembly process to determine the structural and spectral absorbance changes brought about by each additive.[17, 18, 26, 27, 28, 29]

The second part of this thesis focuses on the unusual interaction of Polyethylene Glycol (PEG) with the C8S3 J-aggregate. The original intent of the PEG J-aggregate experiments contained within this section was to create a procedure for infusing fully formed J-aggregates into a polymer film. Theoretically, this would protect the aggregate from the effects of atmospheric oxidative degradation and allow the polymer film to be stretched, aligning the aggregates for directionally dependent microscopy experiments.

The creation of these PEG J-aggregates was designed to mimic the creation procedures of traditional alcoholic route isolated J-aggregates. Observations of the preliminary absorption and emission spectra of these polymer infused J-aggregates revealed dramatic spectral changes with respect to a non-PEG J-aggregate, indicating that changes had occurred within the J-aggregate structure. The J-aggregate solutions which contained PEG concentrations sufficient to make films, did not maintain the UV-Vis

spectral features characteristic of isolated alcoholic route C8S3 J-aggregates. UV-Vis and emission spectra revealed that this PEG J-aggregate procedure could be a new way to study and isolate the inner wall J-aggregate tubule of the double walled C8S3 J-aggregate.

Experimental

Polyethylene Glycol Solutions

Polyethylene glycol (PEG) solutions were made by first creating a 20% wt solution of PEG and 18.3 MΩ water. Polyethylene Glycol (PEG) (Average Mol Wt. 10,000) was purchased from Sigma Aldrich. Once created, this 20% wt stock solution was placed in a bath sonicator for 1 h to insure mixing of the solution. Utilizing this 20% wt PEG stock solution, solutions of 5% wt, 10% wt, and 20% wt PEG were utilized to create PEG J-aggregates. The concentration percentages refer to the weight percent of PEG polymer contained within the water portion of the J-aggregate recipe, as opposed to the total volume. It is important to note that before use, these solutions were sonicated and not shaken. Vigorous shaking infuses the viscous PEG solutions with atmospheric oxygen, causing the rapid oxidation of the C8S3 monomer held within the J-aggregate solution thereby destroying the sample. With respect to the final volume of the J-aggregate samples, the concentrations of PEG in each sample are as follows: 5% PEG = 0.044 g/mL, 10% PEG = 0.088 g/mL, and 20% PEG = 0.177 g/mL.

Creation Method "A" for PEG J-aggregates

Method "A" PEG J-aggregates were created by first placing a 500 μL aliquot of appropriate concentration (5% wt, 10% wt, or 20% wt) PEG solution into a 0.5 dram vial. Next, 130 μL of methanol dispersed C8S3 monomer stock solution 2.92 mM was added to the 0.5 dram vial. The contents of the vial were swirled for 5 seconds and then left to sit in the dark for 24h. An additional 500 μL of the same solution used at the beginning

of this procedure, was then added to the vial. The vial was then swirled and slowly inverted several times until the solution appeared homogeneous. When the sample appeared homogeneous, it was immediately used.

Creation Method "B" for PEG J-aggregates

Method "B" PEG J-aggregates were created by placing a 500 μL aliquot of 18.3 MΩ water into a 0.5 dram vial and adding 130 μL of methanol dispersed C8S3 monomer stock solution 2.92 mM. The contents of the vial were swirled for 5 seconds and left to sit in the dark for 24 h. Next, a 500 μL aliquot of the desired concentration of PEG solution was added to the vial. The vial was then swirled and slowly inverted to homogenize the solution. After homogenization, the sample was used immediately. For simplicity, the method "B" samples are labeled for the final concentration by weight of PEG, with respect to water within the sample vial, as opposed to the concentration that they were created with. The 10% method "B" sample will have the same PEG concentration as the 10% method "A" sample, despite being created using the 20% PEG solution.

Absorption spectra

All PEG J-aggregate absorption spectra were acquired at room temperature using a 0.1 mm path length quartz sample cell and an HP8453A diode array spectrophotometer.

Emission Spectra

All PEG J-aggregate emission spectra were acquired on a Fluorolog 3 fluorimeter, using a 0.1 mm path length quartz sample cell, held in the front faced geometry.

Discussion

Method "A" PEG J-aggregate Absorption

Figure 14 shows absorption spectra for PEG J-aggregates created by method "A" containing varying concentrations of PEG polymer in the sample solution (5% PEG = 0.044 g/mL, 10% PEG = 0.088 g/mL, and 20% PEG = 0.177 g/mL). The 5% PEG method "A" J-aggregates display prominent narrow absorption transitions at the same energy locations as freshly prepared alcoholic route C8S3 J-aggregates, 589 nm outer wall and 599 nm inner wall.[12] This suggests that at low concentrations, the PEG polymer does not interfere with the formation of the double walled tubular structure of the C8S3 J-aggregate. The 10% PEG method "A" J-aggregate absorption spectrum reveals a single prominent narrow transition located at 598 nm, at approximately the same energy location identified as the inner wall tubule of freshly prepared J-aggregates. This would imply that the outer wall of the tube has either never formed, or that the mixing steps of the sample preparation procedure have stripped the outer tube from double walled system with the help of the PEG. The simultaneous solublization of the outer wall and stabilization of the inner wall by the amphiphilic PEG could in part explain these spectral absorbance features. PEG is known to act on proteins in a similar fashion.[30] The 20% PEG method "A" J-aggregate spectrum reveals two prominent transitions, 570 nm and 599 nm. The asymmetric 570 nm transition shares the same absorption energy as transitions known to belong to J-aggregate ribbons or sheets.[18] The low intensity 598 nm transition is indicative of the inner wall tubule of an isolated J-

aggregate. The widely varying absorbance spectra caused by differing amounts of PEG in the presence of aggregating C8S3 monomer, while still maintaining some spectral characteristics of additive free J-aggregates, could lead to a better understanding of this self-assembling system. Further analysis of J-aggregates containing a PEG concentration of 20% or more was deemed unnecessary as high concentrations of PEG appear to have adverse effects on the self aggregation process.

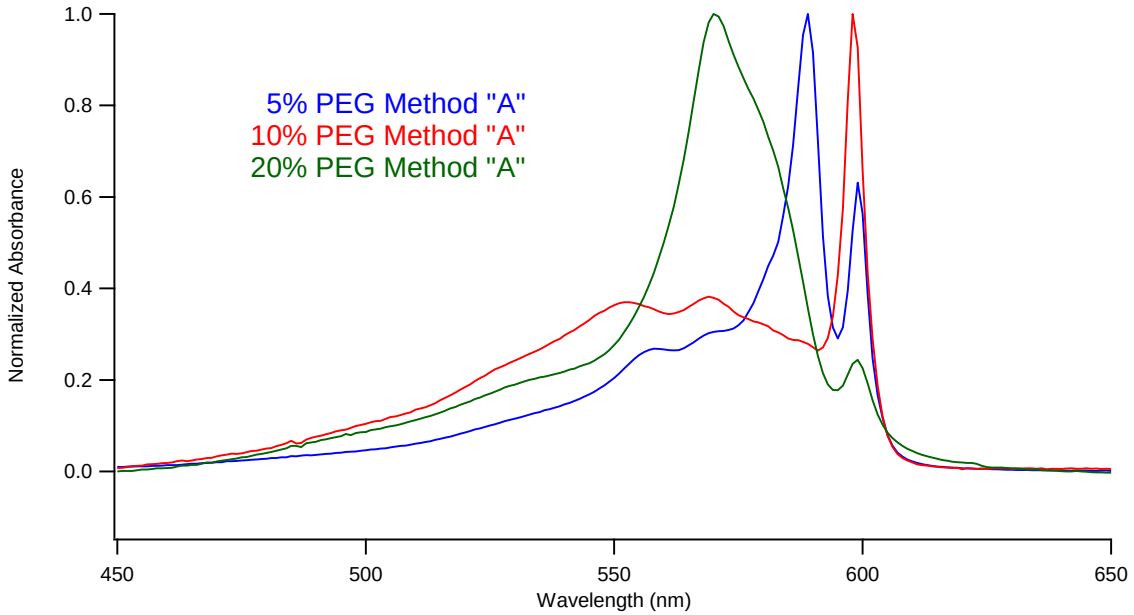

Figure 14. Normalized UV-Vis absorption spectra of freshly created method "A" PEG C8S3 J-aggregate samples created using the following amounts of PEG: 5% = 0.044 g/mL PEG (blue), 10% = 0.088 g/mL PEG (red), and 20% = 0.177 g/mL (green).

Method "B" PEG J-aggregate Absorption

The following experiments were designed to determine the effects of adding PEG to J-aggregates which have already formed. The formation of J-aggregates from monomer takes place during the initial 24 h waiting period immediately following the

addition of monomer to water. The second addition of water is often referred to as the "stabilization step," which dilutes the J-aggregate mixture slowing down the aggregation process. Figure 15 shows absorption spectra of 5% method "B" PEG J-aggregates and 10% method "B" PEG J-aggregates. The 5% PEG method "B" spectrum has two narrow prominent transitions located at 589 nm and 599 nm, the same transition locations belonging to isolated C8S3 alcoholic route J-aggregates. This indicates that small concentrations of PEG do not affect C8S3 alcoholic route J-aggregates that have already formed. The 10% PEG method "B" spectrum displays one prominent narrow transition at 598 nm, similar in energy to transitions which represent the inner wall of alcoholic route PEG free J-aggregates. The simultaneous disappearance of the narrow high energy transition, as compared to non-PEG J-aggregates, and the presence of a narrow low energy transition suggested that the PEG has removed the outer wall of the fully formed J-aggregate while leaving the inner wall intact. Removing the C8S3 monomer from the supramolecular structure of the J-aggregate will disrupt the transition narrowing effect of the ordered monomeric dipoles, thereby removing the high energy transition from the absorbance spectrum. The comparison of the absorption spectra with respect to the method "A" and method "B" PEG J-aggregates revealed identical spectral features among samples with the same concentrations of PEG. There appear to be no absorbance differences with respect to when the PEG is added in the creation process.

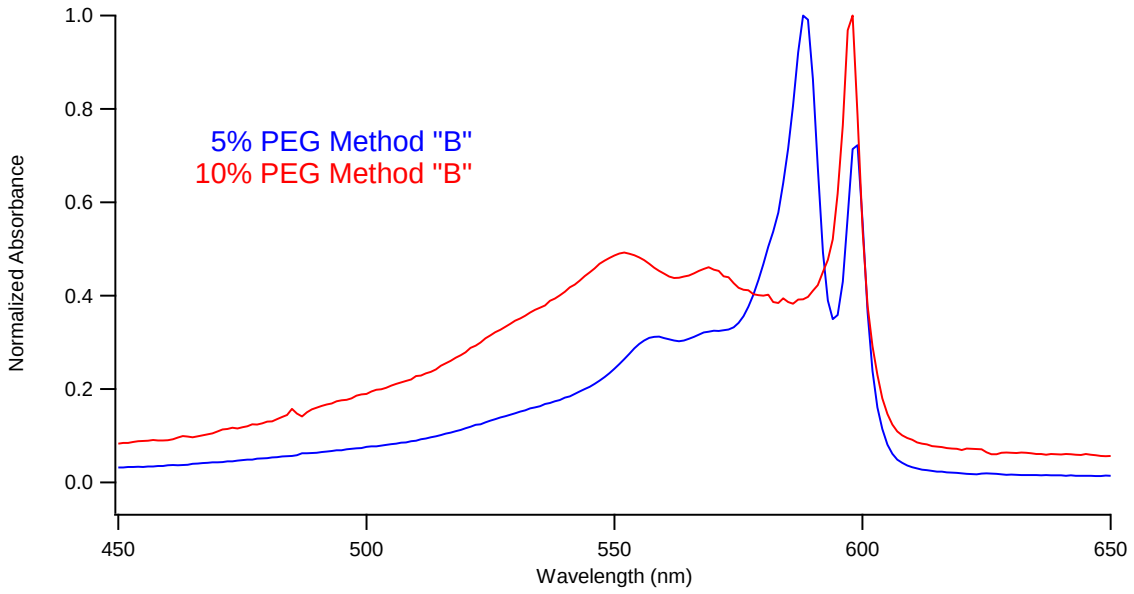

Figure 15. Normalized UV-Vis absorption spectra of method "B" PEG C8S3 J-aggregate samples created using the following PEG concentrations: 5% = 0.044 g/mL (blue) and 10% 0.088 g/mL (red).

The spectra shown in Figure 16 represent non-normalized absorption spectra of a 10% PEG method "A" J-aggregate sample taken at 24 h time intervals after creation of the sample. A comparison of the three spectra reveals that immediately after creation, 0 h, the PEG J-aggregates display a single narrow prominent transition at 598 nm. As time passes, 24 h after the addition of the second aliquot, a high energy narrow transition begins to grow in at 589 nm. After an additional 24 h has passed, 48 h total, the intensity of the high energy transition, located at 589 nm, has become greater than that of the low energy transition, located at 599 nm. It is interesting to note that while the high energy transition has been increasing in intensity, the low energy transition has not changed in absolute absorbance intensity. This suggests that the outer wall of the J-aggregate has

reformed around the pre-existing inner wall. The presence of the high energy tail, 500 – 575 nm, in each absorbance spectrum indicates that the high energy outer wall transition does not contribute to the absorbance of the tail.

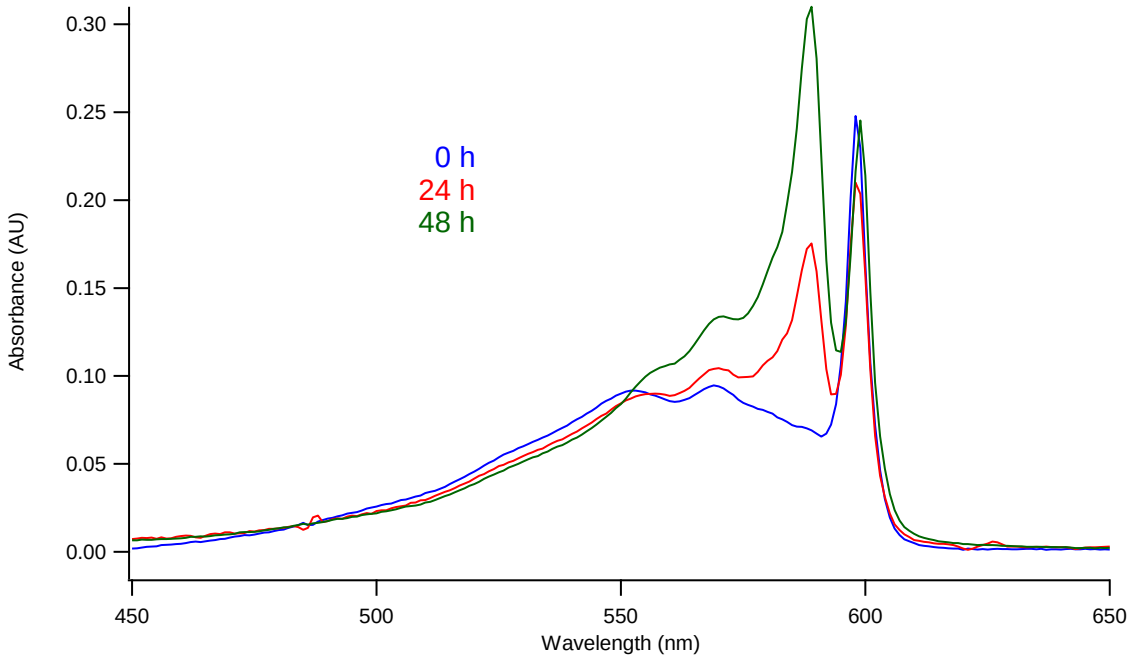

Figure 16. Absolute UV-Vis absorption spectra of a 10% PEG C8S3 J-aggregate sample monitored at 0 h (blue), 24 h (red), and 48 h (green). The high energy peak located at 589 nm can be seen to grow in over a 48 hour period, whereas the low energy peak at 599 nm does not change in intensity.

Fluorescence/ABS

Figure 17 shows a fluorescence emission spectrum of a 10% PEG J-aggregate sample overlaid on top of an absorption spectrum of the same sample. Both spectra were acquired immediately after sample creation. The single emission transition found at 596 nm is similar in energy to the prominent narrow absorption transition found at 598 nm. This 2 nm difference in transition locations is simply a 2 nm variation between the

instruments. The presence of this resonant fluorescence transition indicates that the J-aggregate structure has been maintained. The emission scan range was set to encompass both predominant transitions of isolated alcoholic route J-aggregates, but only the narrow low energy transition representing the inner wall of the J-aggregate was present.

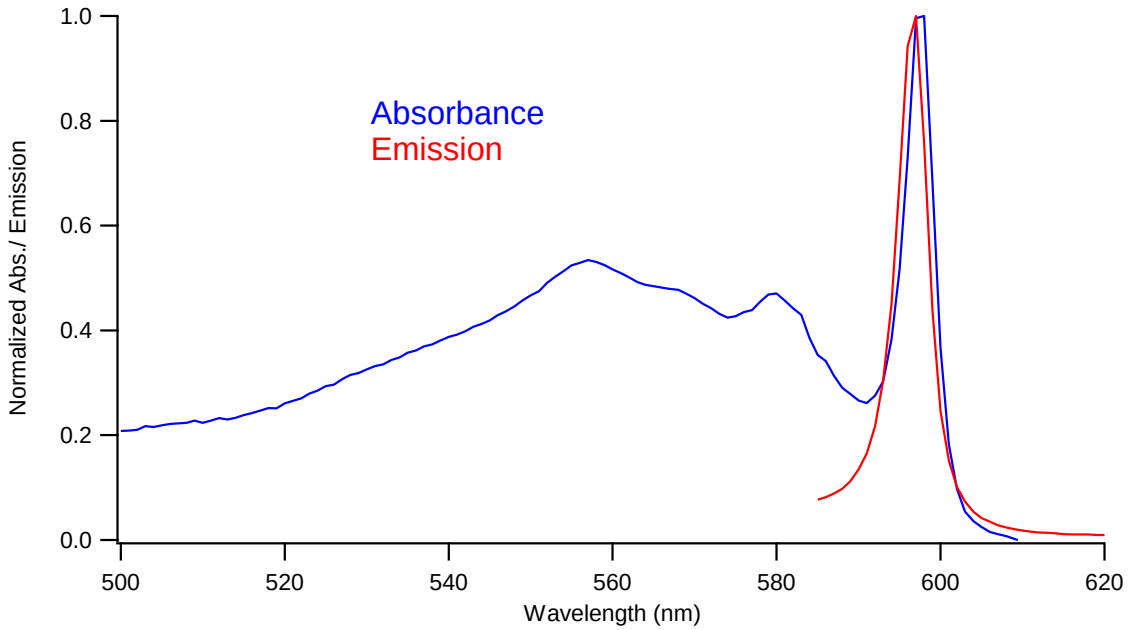

Figure 17. Normalized UV-Vis absorption spectrum (blue) and fluorescence emission spectrum (red) of a freshly created 10% PEG C8S3 J-aggregate sample. The excitation was set to 570 nm.

Conclusions

The work shown in this section has presented a study of the characterization of PEG C8S3 J-aggregates. Initial attempts to create J-aggregate films with PEG have revealed a unique interaction of PEG with the aggregation process C8S3 J-aggregate monomer. Low concentrations of PEG (0.044 g/mL) do not affect the absorbance spectra of alcoholic route C8S3 J-aggregates. C8S3 J-aggregate samples containing PEG concentrations of 0.088 g/mL undergo a reversible loss of the high energy outer wall transition characteristic of alcoholic route C8S3 J-aggregates. The low energy inner wall transition remains after the outer wall has been removed. This high energy transition loss, representing the outer wall, and low energy transition retention, representing the inner wall, was determined by both absorbance and fluorescence spectroscopy. Emission spectra revealed the low energy transition to be in resonance with the absorbance. Spectral features of double walled tubular systems have always been studied as a combination of both the inner wall and the outer wall of the tubule. This is the first time, to our knowledge, that the absorbance spectrum of the inner J-aggregate wall has been captured without any contribution from the outer wall. Confirmation of this claim could be performed using Cryo-TEM, but this technique was not available for this study.

Outlook

The work presented in this section details the study of C8S3 J-aggregates mixed with a PEG additive. Further studies of PEG J-aggregates will allow the identification and characterization of the isolated inner wall aggregate transitions without interference

from the outer wall. Though initial attempts to perform AFM analyses on these PEG J-aggregates were unsuccessful due to dry sample stability; Cryo-TEM analyses could physically confirm the reversible removal of the outer J-aggregate wall, supporting the spectral data. Additionally, the utilization of lower molecular weight PEG in the aggregate creation process will allow the hydrophilic interior of the inner tubule to be probed. Spectral observations of this experiment will lead to the determination of the driving force preserving the inner J-aggregate tubule in its interaction with PEG. As the experiments presented herein are preliminary, further work in this area is needed.

References

(1) Würthner, F.; Kaiser, T. E.; and Saha-Möller, C. R. *Angewandte Chemie International Edition* **2011**, *50*, 3376-3410.

(2) E.E. Jelley, *Nature* **1936**, *138*, 1009-1010.

(3) Kobayashi, T. *J-aggregates*. **1996,** World Scientific: Singapore River Edge, NJ.

(4) Spano, F. C. *Accounts of Chemical Research* **2009**, *43*, 429-439.

(5) De Greef, T. F. A.; Smulders, M. M. J.; Wolffs, M.; Schenning, A. P. H. J.; Sijbesma, R. P.; Meijer, E. W. *Chemical Reviews* **2009**, *109*, 5687 - 5754.

(6) Prokhorenko, V. I.; Steensgaard D. B.; and Holzwarth, A. R. *Biophysical Journal* **2000**, *79*, 2105-2120.

(7) Karrasch, S.; Bullough P. A,; and Ghosh, R. *EMBO Journal* **1995**, *14*, 631-638.

(8) McDermott G.; Prince, S. M.; Freer A. A.; Hawthornthwaite-Lawless, A. M.; Papiz, M. Z.; Cogdell R. J.; and Isaacs, N. W. *Nature* **1995**, *374*, 6522, 517-521.

(9) Augulis, R.; Duppen, K.; Hania, P. R.; Pugzlys, A.; and van Loosdrecht, P. H. M. *International Journal of Photoenergy* **2006**, *2006*,1-9.

(10) Pšenčík, J.; Ma, Y-Z.; Arellano, J.B.; Hála, J.; and Gillbro, T. *Biophysical Journal* **2003**, 84, 1161–1179.

(11) Sundstrom, V.; Gilbro, T.; Gadonas, R.A.; Piskarskas, A. *Journal of Chemical Physics* **1988**, *89*, 2754 – 2762.

(12) Lyon, J. L.; Eisele, D. M.; Kirstein, S.; Rabe, J. P.; Vanden Bout, D. A.; Stevenson, K. J. *Journal of Physical Chemistry C* **2008**, *112*, 1260-1268.

(13) Kirstein, S. and Daehne, S. *International Journal of Photoenergy* **2006**, *2006*, 1-21.

(14) von Berlepsch, H.; Bo1ttcher, C.; Ouart, A.; Burger, C.; Da1hne, S.; Kirstein, S. *Journal of Physical Chemistry B* **2000**, *104*, 5255-5262.

(15) Deisenhofer, J. and Michel, H. *Agnew. Chem.* **1989**, *101*, 872-892.

(16) Hu, X.; Damjanović, A.; Ritz, T.; and Schulten, K. *Proceedings of the National Academy of Sciences USA* **1998**, *95*, 5935-5941.

(17) von Berlepsch, H.; Böttcher, C.; Ouart, A.; Regenbrecht, M.; Akari, S.; Keiderling, U.; Schnablegger, H.; Dähne, S.; and Kirstein, S. *Langmuir* **2000**, *16*, 5908-5916.

(18) von Berlepsch,H.; Kirstein, S.; Hania, R.; Pugžlys, A.; and Böttcher, C. *Journal of Physical Chemistry B* **2007**, *111*, 1701-1711.

(19) von Berlepsch, H.; Kirstein, S.; Hania, R.; Didraga, C.; Pugžlys, A.; and Böttcher, C. *Journal of Physical Chemistry B* **2003**,*107*, 14176-14184.

(20) Scheibe, G.; Schontag, A.; Katheder, F.; *Naturwissenschaften* **1939**, *27*, 499 -501.

(21) Eisele, D. M.; Knoester, J.; Kirstein, S.; Jurgen P. Rabe; and Vanden Bout, D. A. *Nature Nanotechnology* **2009**, *10*, 658-663.

(22) Didraga, C.; Pugzlys, A.; Hania, P. R.; von Berlepsch, H.; Duppen, K.; and Knoester, J. *Journal of Physical Chemistry B* **2004**, *108*, 14976-14985.

(23) Rodger, J. and Nordén, B. *Circular Dichroism and Linear Dichroism*. **1997**, Oxford University Press: Oxford, NY.

(24) Vlaming, S. M.; Bloemsma, E. A.; Nietiadi, M. L.; and Knoester, J. *J. Chem. Phys*. **2011**, *134*,114507 1-11.

(25) Didraga, C.; Klugkist, J.A.; Knoester, J. *Journal of Physical Chemistry B* **2002**, 106, 11474-11486.

(26) Vacha, M.; Saeki, M.; Hashizume, K.; Tani, T. *Chemical Physics* **2002**, 285, 149-155.

(27) von Berlepsch, H.; Regenbrecht, M.; Dähne, S.; Kirstein, S.; and Böttcher, C. *Langmuir* **2002**, *18*, 2901-2907.

(28) von Berlepsch, H.; Kirstein, S.; and Böttcher, C. *Journal of Physical Chemistry B* **2003**, *107*, 9646-9654. (28)

(29) Gao, J.; Kamps, A.; Park, S.-J.; and John K. Grey, J. K. *Langmuir* **2012**, http://pubs.acs.org on October 31, 2012.

(30) Rajan, R.S.; Li, T.; Aras, M.; Sloey, C.; Sutherlan, W.; Arai, H.; Briddell, R.; Kinstler, O.; Lueras, A. M. K.; Zhang, Y.; Yeghnazar, H.; Treuheit, M.; and Brems, D. N. *Protein Science* **2006**, *15*,1063-1075.